Himalayan Physics

First-principles DFT study of the molecular structure, spectroscopic analysis, electronic structures, and thermodynamic properties of ascorbic acid

https://doi.org/10.3126/hp.v11i1.65329

Pima Gharti Magar, Roshika Uprety, Krishna Bahadur Rai*

Department of Physics, Patan Multiple Campus, Lalitpur, Tribhuvan University, Nepal

Abstract: We comprehensively analyzed ascorbic acid using density functional theory at B3LYP/6-311G(d,p) level of theory. Vibrational analysis revealed various modes, including C-C and C-H stretching and in-plane C-H bending vibrations within the 3000-3100 cm^{-1} range. Examining HOMO-LUMO energy provided insights into chemical stability with an energy gap of 5.65 eV. The compound with such a higher HOMO-LUMO gap is comparatively harder. The density of states spectrum with an energy gap of 5.63 eV supplemented our HOMO-LUMO analysis by elucidating orbital energy levels. The calculated hardness, at 2.82 eV, reflects the molecule's stability and resistance to electron density changes. With a chemical potential of -3.98 eV, indicating the potential energy of the substance, a more negative value suggests a higher propensity for the molecule to undergo reactions or release energy. The electronegativity value of 3.98 eV signifies the molecule's or atom's ability to attract electrons in a chemical bond. A softness value of 0.34 eV^{-1} denotes the molecule's polarizability and ease of electron transfer. Furthermore, the electrophilicity index of 2.81 eV suggests its electrophilic character, indicating its capability to accept electrons in chemical reactions. Visualizations of ESP, MEP, and ED enhanced the understanding of molecular interactions and charge distribution. Mulliken charges analysis highlighted regions of positive and negative charge localization, with C1 and O8 atoms exhibiting the highest positive and negative charges, respectively. Thermodynamic properties such as heat capacities, internal energy, enthalpy, and entropy increased with temperature, contrasting with the trend observed for Gibbs free energy, providing insights into the molecule's behavior under different temperature conditions.

Keywords: Ascorbic acid • Density functional theory • Vibrational analysis • Electronic structures • Thermodynamic parameters

Recieved: 2024-05-01 **Revised: 2024-05-17** **Published: 2024-05-31**

I. Introduction

Ascorbic acid is an organic compound that belongs to a group of organic substances called butenolides. These are dihydrofurans where the carbonyl group is attached to the carbon atom, i.e., at position

* *Corresponding Author: krishnarai135@gmail.com*

C2 in Fig. 1(a). Vitamins are essential for the body to various processes. The two types of vitamins are water-soluble (vitamin C) and fat-soluble (vitamins K, E, D, and K). Ascorbic acid ($C_6H_8O_6$), or vitamin C, is an antioxidant that dissolves in water. Hungarian biochemist and Nobel Prize laureate Szent-Gyor Gyi isolated it for the first time in 1928 [1]. Ascorbic acid can be found in citrus fruits, strawberries, tomatoes, turnips, watermelon, pineapple, papaya, mango, and other leafy vegetables. A small amount of vitamin C is also found in fish and milk. It helps to lower blood cholesterol and shields the body against the damaging effects of pollution and free radicals. Both tissue growth and wound healing require it. A lack of this vitamin can result in infections, scurvy, anemia, and poor wound healing [2]. The chemical structure of ascorbic acid includes the arrangement of carbon, hydrogen, and oxygen atoms and their chemical bonds that hold the atoms together. Bichara studied the Density Functional Theory (DFT) calculation of the molecular force field of L-ASCORBIC acid, vitamin C, together with IR spectroscopic techniques for both solid and aqueous solution phases and found that stable conformation of L-ASCORBIC acid in both solid and gas phases [3]. Nuclear magnetic resonance, Raman spectroscopy [4], and DFT were employed to analyze the spectra, structure, and antioxidant activity of ascorbic acid, which offers a view into its spectroscopic, structural, and antioxidant properties, particularly in aqueous phases, thus contributing significantly to the understanding and potential health benefits of it [5]. Monte Carlo simulations were performed on pure liquid water and the dilute aqueous solution of Vitamin C molecules, and they confirmed the different properties, such as the distribution of several water ring structures and the free energy of the solution [6]. Yamabe conducted a DFT investigation on the transition state and frontier orbitals in L-ASCORBIC acid oxidation and degradation, revealing insights into OH addition and identifying proton transfers with minimal energy in transition states of intermediate carboxylic acids, alongside recognizing participating side-chain reactions [7].

The equilibrium configuration, vibrational analysis, electronic structures, and thermodynamic properties of ascorbic acid have never been studied before using the DFT first-principles analysis with the basis set 6-311G (d, p). Hence, research on this topic is vital. So, we study to find the optimized structure, optimization steps and its energy, vibrational analysis, highest occupied molecular orbitals (HOMO) and lowest unoccupied molecular orbital (LUMO) analysis, global reactivity parameters, electrostatic potential (ESP) surfaces, molecular electrostatic potential (MEP), electron density (ED), density of states (DOS), Mulliken atomic charges and thermodynamic properties of the ascorbic acid molecule using DFT with B3LYP/6-311G(d, p) level of theory.

II. Computational Methodology

All the quantum mechanical calculations on ascorbic acid were carried out via the Gaussian 09W [8] using the DFT/B3LYP method and 6-311G(d, p) basis set. The molecular structures were visualized

using GaussView software [9]. The optimized structural parameters were used in the vibrational frequency calculations to characterize the mode of vibrations together with HOMO-LUMO, MEP, ESP, and ED. The GaussSum 3.0 program was used to observe the DOS spectrum [10]. The optimization output frequency file obtained from the Gaussian calculation was used to calculate the thermodynamic parameters by employing the Moltran program [11].

For the determination of global reactivity parameters such as chemical hardness (η), electronic chemical potential (μ), electronegativity (χ), softness (S), and electrophilicity index (ω), we use Koopman's theorem. The ionization potential (I) and electron affinity (A), respectively, have a direct relationship with the energies of HOMO and LUMO [12],

$$I = -E_{HOMO} \tag{1}$$

$$A = -E_{LUMO} \tag{2}$$

In Koopman's theorem for closed-shell molecules [13], let N and E stand for electron count and total energy, respectively. The ratio of the second-order derivative of the total energy (δE) system to the change in the number of electrons (δN) indicates the chemical hardness (η) of the system [14]. Mathematically, it is written as

$$\eta = \frac{1}{2}\frac{\delta^2 E}{\delta^2 N} \tag{3}$$

On solving, we get,

$$\eta = \frac{1}{2}(I - A) \tag{4}$$

Potential energy generated or absorbed during a chemical reaction can be determined using quantum chemical characteristics like electronic chemical potential (μ) and electronegativity (χ). Here, the equation for the chemical potential (μ) is obtained by the ratio of the first derivative of energy (δE) to the number of electrons (δN) [15], and it is

$$\mu = \frac{\delta E}{\delta N} \tag{5}$$

Then, it can be simplified as,

$$\mu = -\frac{1}{2}(I + A) \tag{6}$$

The chemical potential (μ) obtained from the above expression is equal to the negative of the electronegativity (χ) such that $\mu = -\chi$. Therefore,

$$\chi = \frac{1}{2}(I + A) \tag{7}$$

Similarly, the softness (S) [16] is given by,

$$S = \frac{1}{\eta} \tag{8}$$

And electropositivity or electrophilicity index (ω) [17] is given by,

$$\omega = \frac{\mu^2}{2\eta} \tag{9}$$

III. Results and Discussion

Optimized molecular structure and optimization steps

Fig. 1(a) displays the optimized molecular structure of the ascorbic acid with atomic numbering and its symbol using DFT at B3LYP/6-311G(d, p) basis set. Fig. 1(b) shows the total number of optimization steps vs the total energy, and this molecule obtains the optimized molecular structure at 11 different steps. The total energy of the initial structure is -18632.21 eV (-684.72 Hartree). After 11 optimization steps, the ground state energy of the optimized ascorbic acid attains -18632.22 eV (-684.72 Hartree) value.

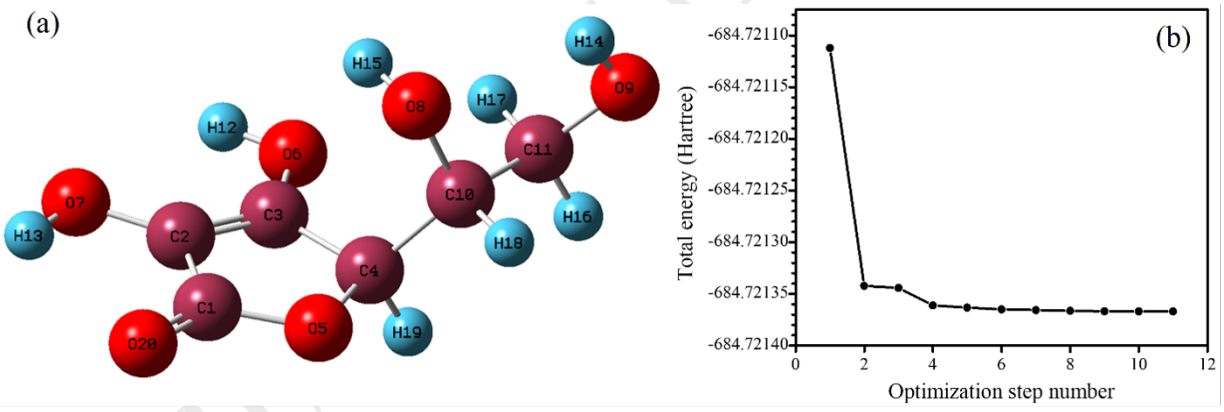

Figure 1. (a) Optimized molecular structure of ascorbic acid with the numbering and symbol of atoms, (b) Plot for optimization step number vs total energy.

Vibrational analysis of ascorbic acid molecule

Infrared (IR) spectra of a neutral ascorbic acid molecule are shown in Fig. 2. In the IR graph, the horizontal line illustrates the wavenumber, and the vertical line represents the percentage of light transmitted. This depicts the correlation between the frequency (or wavenumber) and wavelength of infrared light, showcasing either transmittance or absorption characteristics [18–20]. When energy is low, absorption is high. By observing IR spectra, the modes of vibrations can be studied. The vibration modifies the polarizability or dipole moment of the molecule based on whether the molecule is Raman or IR active, respectively [21]. In ascorbic acid, major modes of vibrations like stretching, rocking, and scissoring, as well as symmetric and asymmetric mode for C-H bonds, have been seen.

C- H vibrations

Aromatic compounds have multiple weak bands in the 3100–3000 cm^{-1} region due to aromatic C–H stretching vibrations [22, 23]. Here in our molecule, the C-H stretching vibrations are detected at 3016.07 cm^{-1} and 3040.68 cm^{-1}.

C- C vibrations

The region where the ring carbon-carbon stretching vibrations are investigated is 1625–1430 cm^{-1} [24, 25]. In this instance, the ring's C-C stretching vibration bands are visible at 1435.26 cm^{-1}, 1444.13 cm^{-1}, and 1450.38 cm^{-1} in the FT-IR spectrum.

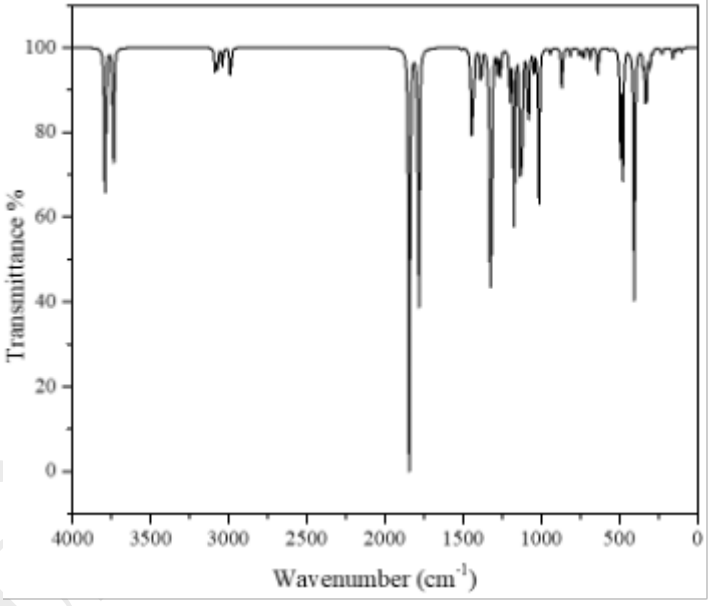

Figure 2. FT-IR-spectra of ascorbic acid using the DFT method.

HOMO –LUMO analysis

Fig. 3 shows the HOMO-LUMO diagram. The HOMO orbitals are the electrophilic portion that has the propensity to give electrons away. In contrast, the LUMO orbitals are the nucleophilic portion that inclines to either gain or receive electrons. After optimizing the molecular structure, the HOMO-LUMO gap is calculated. The highest occupied and lowest unoccupied orbitals are vital in finding chemical stability [26]. The HOMO and LUMO energies are utilized to calculate the energy gap (ΔE), which provides details about the structure's chemical stability and reactivity [27–29]. Fig. 3 shows the HOMO = - 6.81 eV and LUMO = - 1.16 eV. Both the HOMO and LUMO energies are negative, signifying their stable nature. The ascorbic acid's energy gap (ΔE) is 5.65 eV, highlighting its stability.

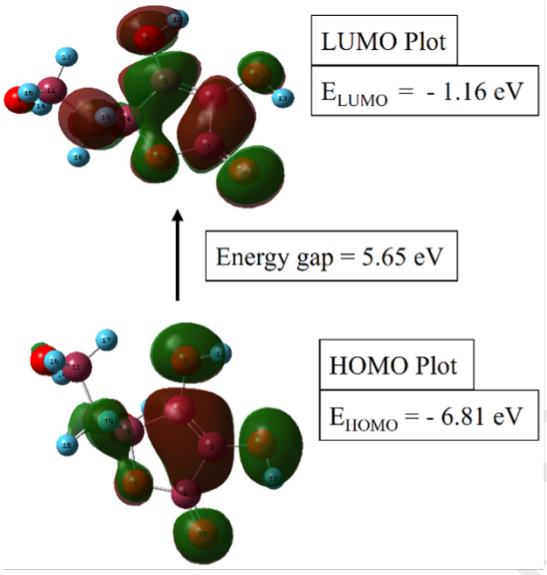

Figure 3. HOMO and LUMO orbitals of ascorbic acid.

Global reactivity parameters

In any molecule, their HOMO and LUMO correspond to the ionization potential (I) and electron affinity (A) respectively. The global reactivity indices include hardness (η), chemical potential (μ), softness (S), electronegativity (χ), and electropositivity (ω) [30], and these have been defined based on the energy values of a molecule's HOMO and LUMO [31]. The smallest amount of energy needed to remove an electron to infinity from an atom or molecule in its gaseous form is known as the ionization energy (I). Conversely, electron affinity (A) is the energy released when an electron is added to a neutral atom or molecule in a gaseous state to generate a negative ion. The values of I and A are found to be 6.81 eV and 1.16 eV, respectively.

The chemical hardness is related to the stability and reactivity of the chemical system [32]. The HOMO-LUMO gap is larger in hard molecules and smaller in soft molecules. Using the equations from (1) to (7), we calculate the global reactivity parameters and found the values for chemical hardness (η) = 2.82 eV, chemical potential (μ) = -3.98 eV, electronegativity (χ) = 3.98 eV, chemical softness (S) = 0.34 eV^{-1} and electrophilicity index (ω) = 2.81 eV. The calculated hardness of 2.82 eV shows the molecule's stability and resistance to the change in electron density. A chemical potential value of -3.98 eV measures the potential energy of the substance, and a more negative value suggests that the molecule is more prone to react or release energy. An electronegativity value of 3.98 eV indicates the ability of a molecule/atom to attract electrons in a chemical bond. Chemical softness is the inverse of global hardness and represents the ease with which a molecule can accept or donate electrons. The softness value of 0.34 eV^{-1} means its polarizability and ease of electron transfer. The electrophilicity index of 2.81 eV suggests its electrophilic

character, which means it can accept electrons in chemical reactions.

Electrostatic potential (ESP) surfaces, Molecular electrostatic potential (MEP), and Electron density (ED)

Fig. 4(a) shows the ESP surface with values ranging from -1.441e-2 a.u. (red) to +1.441e-2 a.u. (blue). The energy of a positive charge interacting with the electrons and nuclei of a molecule is termed the electrostatic potential. The red color suggests a higher negative charge, while the blue color indicates a higher positive charge. For ESP, as shown in Fig. 4(a), the negative potential is hanging out around the oxygen because it is more prone to electrophilic attacks, showing up as a yellowish region, and the rest of the surface is localized with positive potential, signaling its inclination for nucleophilic attacks.

Fig. 4(b) shows the MEP surface map in the range of -7.556e-2 a.u. (red) to +7.556e-2 a.u. (blue). The MEP correlates with dipole moments, electro negativity, partial charges, and chemical reactivity of the molecule. It indicates the net electrostatic effect produced at a point in the space surrounding a molecule by its total charge distribution (electron + nuclei) [33]. It provides a visual method to understand the relative polarity of the molecule. Oxygen atoms exhibit slightly negative MEP, especially when bonded to other carbon atoms or hydrogen, and hydrogen atoms show the negative region of MEP.

The ED map shows the probability of an electron being present at a specific location (Fig. 4(c)). The size, shape, charge density, and reactive sites of the molecules are shown by an electron density surface map using an electrostatic potential surface.

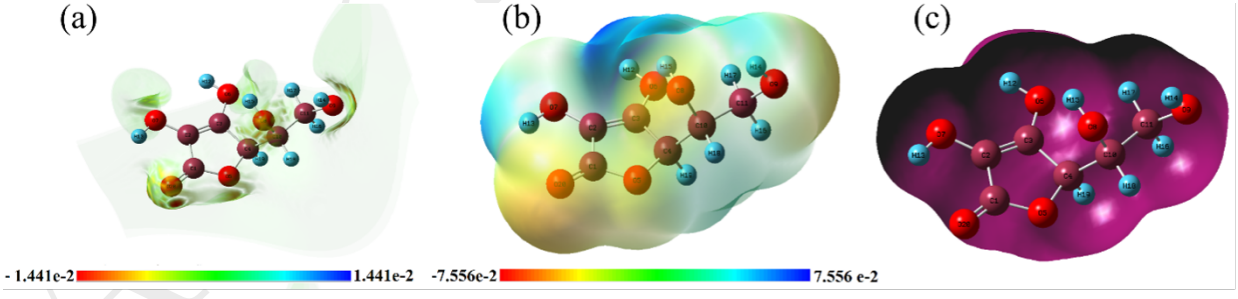

Figure 4. (a) Electrostatic potential, (b) Molecular electrostatic potential, and (c) Electron density, of ascorbic acid.

Density of states (DOS)

Just taking into account HOMO and LUMO may not give a meaningful representation of the frontier orbitals because the boundary areas of nearby orbitals may exhibit quasi-degenerate energy levels [34]. Because of this, we observe the DOS using the GaussSum 3.0 software. The DOS graph clarifies whether the two orbitals have an anti-bonding or bonding connection. Fig. 5 shows the energy gap from the DOS spectrum, equal to 5.63 eV. The energy gap shown in this DOS spectrum agrees well with the energy

gap value reported in the HOMO-LUMO study.

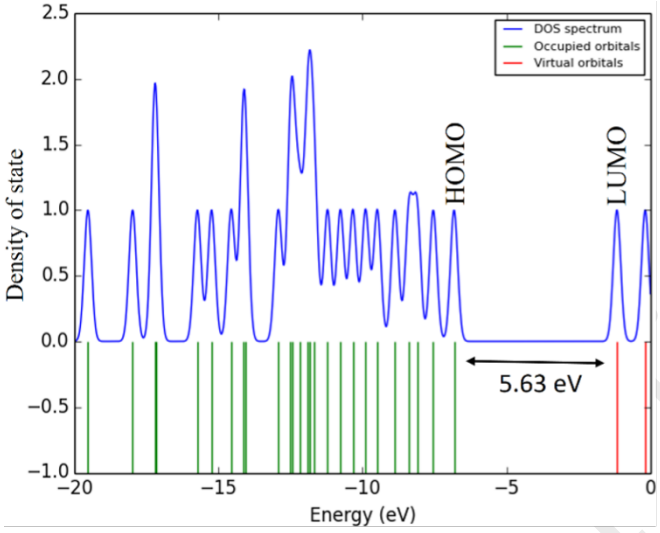

Figure 5. Density of states (DOS) spectrum of ascorbic acid molecule.

Mulliken atomic charges

Mulliken charge calculations are essential in quantum chemistry since they affect polarizability, electronic structure, dipole moment, and other molecular properties [35, 36]. The calculated data of Mulliken atomic charges are shown in histogram of Fig. 6. It can be observed that C1, C2, C3, C4, C11, H12, H14, H15, H16, H17, H18, and H19 atoms of $C_6H_8O_6$ perform positive charges and O5, O6, O7, O8, O9, O20 and C10 show the negative charges. Among them, it is clear that the C1 and O8 atoms have the highest positive and negative charges, respectively.

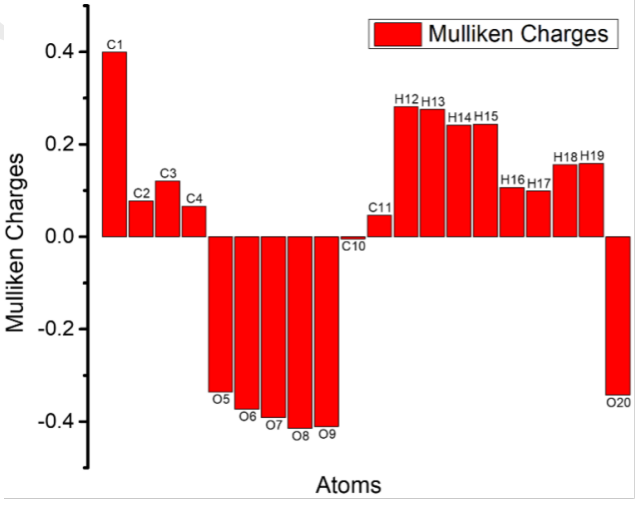

Figure 6. Mulliken charges distribution chart of the ascorbic acid molecule.

Thermodynamics analysis

The thermodynamic parameters, including heat capacity at constant volume (Cv), heat capacity at constant pressure (Cp), total internal energy (U), enthalpy (H), entropy (S), and Gibbs free energy (G), are observed using the Moltran software. Fig. 7(a) and Fig. 7(b) show the heat capacity as a function of temperature at constant volume and pressure, respectively. Both graphs show a linear monotonic rise in the heat capacity with the temperature increase.

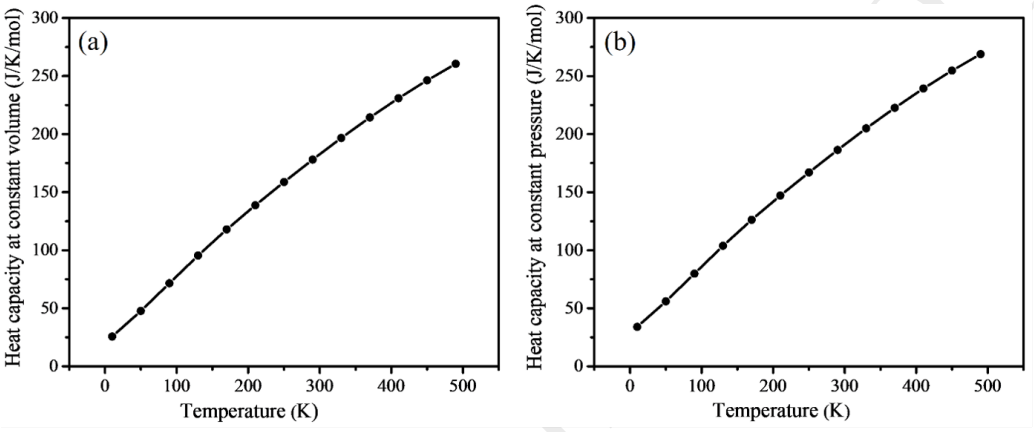

Figure 7. Heat capacity at (a) Constant volume and (b) Constant pressure of ascorbic acid as a function of temperature.

Fig. 8(a) depicts the behavior of internal energy versus temperature, while Fig. 8(b) shows the behavior of enthalpy versus temperature. These figures show that as the temperature rises, the internal energy and enthalpy of the molecule increase in a similar trend.

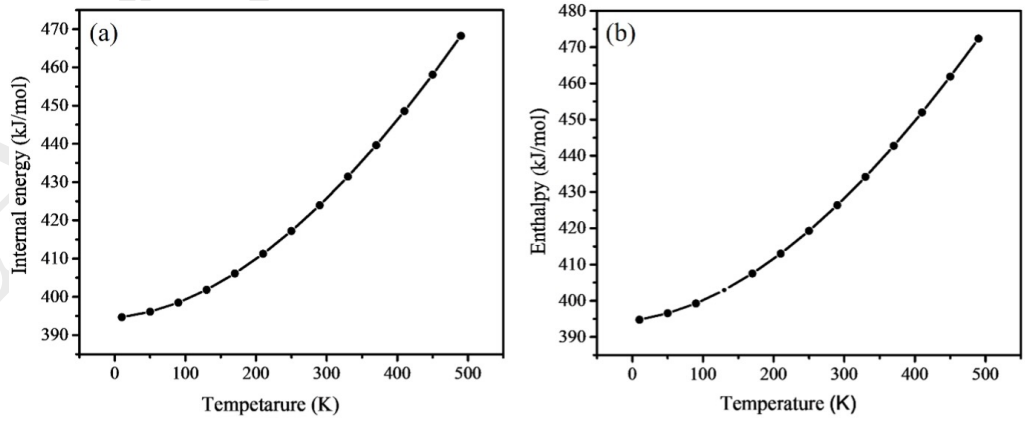

Figure 8. Temperature dependence of (a) Internal energy and (b) Enthalpy of ascorbic acid.

Fig. 9(a) presents the graph of entropy with respect to the temperature. It clearly shows that the entropy increases with the temperature rise. Fig. 9(b) shows the temperature dependence of Gibbs free

energy of ascorbic acid. It shows that Gibbs's energy decreases with an increase in temperature.

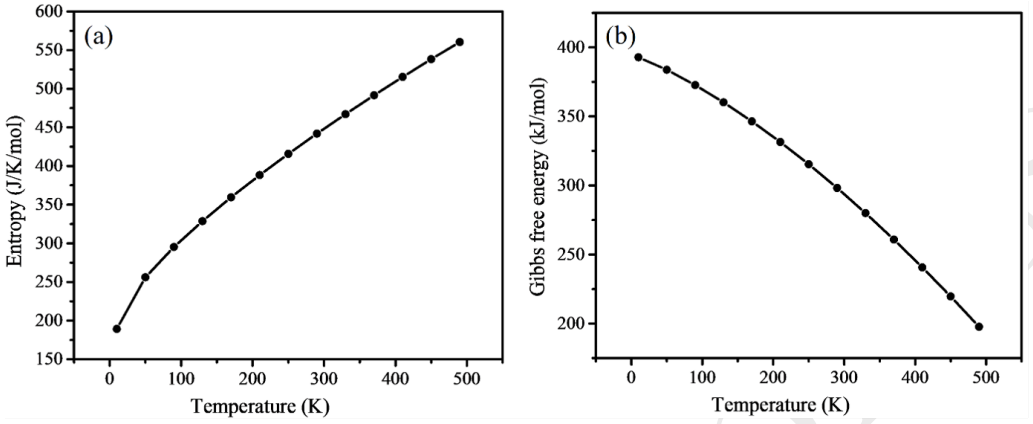

Figure 9. Temperature dependence of (a) Entropy and (b) Gibb's free energy of ascorbic acid.

The system's overall energy change, or entropy, must be positive. Additionally, the system's enthalpy change must be negative, meaning that the enthalpy term must be less than the entropy term, causing Gibbs free energy to become negative [37]. The graphs from Fig. 7(a), Fig. 7(b), Fig. 8(a), Fig. 8(b), and Fig. 9(a), illustrate how thermodynamic parameters such as heat capacity at constant volume (Cv), heat capacity at constant pressure (Cp), total internal energy (U), enthalpy (H) and entropy (S) increase as the temperature rises due to the increase in molecular vibrational intensities.

IV. Conclusion

The first-principles DFT/B3LYP method with a 6-311G (d, p) basis set was used to determine the molecular structure, spectroscopic analysis, electronic structures, and thermodynamic properties of the ascorbic acid molecule. We optimized the molecular structure of ascorbic acid and explored its vibrational modes, including C-H and C-C vibrations, elucidating its spectral characteristics. Its C-H vibrations are located in the 3100–3000 cm^{-1} region for C–H vibration (i.e., 3016.07 and 3078.55 cm^{-1}). Similarly, the 1625–1430 cm^{-1} region is identified for ring carbon-carbon stretching. We conducted a thorough analysis of the HOMO and LUMO, revealing insights into its chemical stability and reactivity. From the observation value of HOMO and LUMO, the energy gap was found to be 5.65 eV. The energy gaps observed in the HOMO-LUMO and DOS spectrums are equivalent and correspond well. The DOS spectrum provided additional clarity on the energy levels of orbitals, complementing our HOMO-LUMO analysis. The global reactivity parameters, including hardness, chemical potential, electronegativity, chemical softness, and electrophilicity index, were found to be 2.82 eV, -3.98 eV, 3.98 eV, 0.34 eV^{-1}, and 2.81 eV, respectively suggesting valuable information on its chemical reactivity and interaction potential. Visualizations of electrostatic potential surfaces, molecular electrostatic potential, and electron density offered a deeper

understanding of its molecular interactions and charge distribution. Mulliken charge analysis shows that all the hydrogen and carbon atoms except C10 exhibit a positive charge. In contrast, all the oxygen atoms and C10 display a negative charge, emphasizing key regions of positive and negative charge localization. Gibbs free energy decreases as temperature rises, while heat capacity at constant volume (Cv) and pressure (Cp), internal energy (U), enthalpy (H), and entropy (S) increase with the same rise in temperature, providing insights into the molecule's behavior under different conditions.

References

[1] Iqbal K, Khan A, Khattak M. Biological significance of ascorbic acid (vitamin C) in human health-a review. Pakistan Journal of Nutrition. 2004;3(1):5-13.

[2] Griffiths JK. Vitamin deficiencies. In: Hunter's tropical medicine and emerging infectious diseases. 10th ed. Elsevier; 2020. p. 1042-7.

[3] Bichara LC, Lanus HE, Nieto CG, Brandan SA. Density functional theory calculations of the molecular force field of L-ascorbic acid, vitamin C. The Journal of Physical Chemistry A. 2010;114(14):4997-5004.

[4] Rai KB, Yadav RP. Raman spectroscopy investigation on semi-curve woven fabric-graphene synthesized by the chemical vapor deposition process. Jordan Journal of Physics. 2022;15(2):169-77.

[5] Singh G, Mohanty BP, Saini GSS. Structure, spectra, and antioxidant action of ascorbic acid were studied by density functional theory, Raman spectroscopic, and nuclear magnetic resonance techniques. Spectrochimica Acta Part A: Molecular and Biomolecular Spectroscopy. 2016;155:61-74.

[6] Gauli HRK, Rai KB, Giri K, Neupane R. Monte-Carlo simulation of phase transition in 2d and 3d Ising model. Scientific World. 2023;16(16):12-20.

[7] Yamabe S, Tsuchida N, Yamazaki S, Sakaki S. Frontier orbitals and transition states in the oxidation and degradation of l-ascorbic acid: a DFT study. Organic and Biomolecular Chemistry. 2015;13(13):4002-15.

[8] Frisch MJ, Trucks GW, Schlegel HB, Scuseria GE, Robb MA, Cheeseman JR, et al.. Gaussian Inc., Wallingford, CT; 2009.

[9] Frisch HP, Hratchian RD, Dennington TA, Keith J, Millam AB, Nielsen A, et al.. Gauss View, Version 5.08; 2009.

[10] O'Boyle NM, Tenderholt AL, Langner KM. cclib: A library for package-independent computational chemistry algorithms. Journal of Computational Chemistry. 2008;29(5):839-45.

[11] Ignatov SK. Moltran v. 2.5-Program for molecular visualization and thermodynamic calculations; 2004.

[12] Parida SK, Behera D, Sahu S. A computational quantum chemical and polarizability calculations of

liquid crystal 4-cyano-4-pentylbiphenyl with a water molecule (H2O). Journal of Molecular Structure. 2021;1227:129568-72.

[13] Koopmans T. Uber die Zuordnung von Wellenfunktionen und Eigenwerten zu den Einzelnen Elektronen Eines Atoms. Physica. 1934;1(1–6):104-13.

[14] El-Mansy MAM, Ibrahim M, Suvitha A, Abdelsalam H, Osman W. Boosted electronic, optical, and NLO responses of homo P-nanoclusters via conducting polymeric substituents. Computational and Theoretical Chemistry. 2021;1202:113343-7.

[15] Rajesh P, Gunasekaran S, Gnanasambandan T, Seshadri S. Molecular structure and vibrational analysis of Trifluoperazine by FT-IR, FT-Raman, and UV–Vis spectroscopies combined with DFT calculations. Spectrochimica Acta Part A: Molecular and Biomolecular Spectroscopy. 2015;137:1184-93.

[16] El-Mansy MAM, El-Bana MS, Fouad SS. On the spectroscopic analyses of 3-Hydroxy-1-PhenylPyridazin-6(2H)one (HPHP): A comparative experimental and computational study. Spectrochimica Acta Part A: Molecular and Biomolecular Spectroscopy. 2017;176:99-105.

[17] El-Mansy MAM. Quantum chemical studies on structural, vibrational, nonlinear optical properties and chemical reactivity of indigo carmine dye. Spectrochimica Acta Part A: Molecular and Biomolecular Spectroscopy. 2017;183:284-90.

[18] Khan SA, Khan SB, Khan LU, Farooq A, Akhtar K, Asiri AM. Fourier transform infrared spectroscopy: fundamentals and application in functional groups and nanomaterials characterization. In: Handbook of materials characterization. Springer, Cham; 2018. p. 281-303.

[19] Kohn W. Nobel Lecture: Electronic structure of matter-wave functions and density functionals. Reviews of Modern Physics. 1999;71(5):1253.

[20] Rai KB, Yadav RP, Shrestha PM, Gupta SP, Neupane R, Ghimire RR. Fabrication of gas sensor based on graphene for the adsorption of gases produced from waste material in kitchen and its surrounding. Journal of Nepal Physical Society. 2022;8(3):26-31.

[21] Karabacak M, Sinha L, Prasad O, Cinar Z, Cinar M. The spectroscopic (FT-Raman, FT-IR, UV and NMR), molecular electrostatic potential, polarizability and hyperpolarizability, NBO and HOMO–LUMO analysis of monomeric and dimeric structures of 4-chloro-3, 5-dinitrobenzoic acid. Spectrochimica Acta Part A: Molecular and Biomolecular Spectroscopy. 2012;93:33-46.

[22] Varsányi G. Assignments for vibrational spectra of 700 benzene derivates. Akademiai Kiado; 1973.

[23] Limbu S, Ojha T, Ghimire RR, Rai KB. An investigation of vibrational analysis, thermodynamics properties and electronic properties of Formaldehyde and its stretch by substituent acetone, acetyl chloride and methyl acetate using first principles analysis. BIBECHANA. 2024;21(1):23-36.

[24] Sundaraganesan N, Joshua BD, Meganathan C, Sebastian S. Vibrational spectroscopic studies supported by HF/DFT calculations of 2, 4, and 6-thiamin pyrimidine. Indian Journal of Chemistry.

2008;47A:821-9.

[25] Ojha T, Limbu S, Shrestha PM, Gupta SP, Rai KB. Comparative Computational Study on Molecular Structure, Electronic and Vibrational Analysis of Vinyl Bromide based on HF and DFT Approach. Himalayan Journal of Science and Technology. 2023;7(1):38-49.

[26] Miar M, Shiroudi A, Pourshamsian K, Oliaey AR, Hatamjafari F. Theoretical investigations on the HOMO–LUMO gap and global reactivity descriptor studies, natural bond orbital, and nucleus-independent chemical shifts analyses of 3-phenylbenzo[d]thiazole-2(3H)-imine and its para-substituted derivatives: Solvent and substituent effects. Journal of Chemical Research. 2021;45(1–2):147-58.

[27] Padmaja L, Ravikumar C, Sajan D, Hubert Joe I, Jayakumar VS, Pettit GR, et al. Density functional study on the structural conformations and intramolecular charge transfer from the vibrational spectra of the anticancer drug combretastatin-A2. Journal of Raman Spectroscopy. 2009;40(4):419-28.

[28] Ravikumar C, Joe IH, Jayakumar VS. Charge transfer interactions and nonlinear optical properties of push–pull chromophore benzaldehyde phenylhydrazone: a vibrational approach. Chemical Physics Letters. 2008;460(4–6):552-8.

[29] Rai KB, Khadka IB, Koirala AR, Ray SK. Insight of cleaning, doping and defective effects on the graphene surface by using methanol. Advances in Materials Research. 2021;10(4):283-92.

[30] Devi D, Arasu MMA, Girija AM. Spectroscopic (FTIR, UV-Vis, NMR) investigations, DFT predictions of global reactivity descriptors and efficient corrosion inhibitors of N-carbobenzoxy-L-ValineSuccinimidyl Ester. Journal of the Indian Chemical Society. 2022;99(4):100400-16.

[31] Chattaraj PK, Maiti B, Sarkar U. Publicity: a unified treatment of chemical reactivity and selectivity. The Journal of Physical Chemistry A. 2003;107(25):4973-5.

[32] Pratiwi R, Ibrahim S, Tjahjono DH. Reactivity and Stability of Metalloporphyrin Complex Formation: DFT and Experimental Study. Molecules. 2020;25(18):4221.

[33] Nkungli NK, Ghogomu JN. Theoretical analysis of the binding of iron (III) protoporphyrin IX to 4-methoxyacetophenone thiosemicarbazone via DFT-D3, MEP, QTAIM, NCI, ELF, and LOL studies. Journal of Molecular Modeling. 2017;23:1-20.

[34] Brinck T, Stenlid JH. The molecular surface property approach: a guide to chemical interactions in chemistry, medicine, and material science. Advanced Theory and Simulations. 2019;2(1):1800149.

[35] Mulliken RS. Electronic population analysis on LCAO-MO molecular wave functions. The Journal of Chemical Physics. 1955;23:1833-40.

[36] Rai KB, Ghimire RR, Dhakal C, Pudasainee K, Siwakoti B. Structural Equilibrium Configuration of Benzene and Aniline: A First-Principles Study. Journal of Nepal Chemical Society. 2024;44(1):1-15.

[37] Ott JB, Boerio-Goates J. Chemical Thermodynamics: Advanced Applications. California: Academic Press; 2000.